

# Weldability of High Strength Aluminum Alloys by Friction Stir Welding

Kazuhiro NAKATA<sup>1)</sup>, Young Gon KIM<sup>1)</sup>, Masao USHIO<sup>1)</sup>, Takenori HASHIMOTO<sup>2)</sup> and Shigetoshi JYOGAN<sup>2)</sup>

1) Joining and Welding Research Institute, Osaka University, 11-1, Mihogaoka, Ibaraki, Osaka 567-0047 Japan

2) Research Laboratory, Showa Aluminum Corporation, 480, Inuzuka, Oyama, Tochigi 323-8678 Japan

The effects of welding conditions, tool rotation speed,  $Rt$  and plate traveling speed,  $V$  on weld joints formation and mechanical properties have been investigated on Friction Stir Welding joints of high strength aluminum alloys of 2024-T6 and 7075-T6 in comparison with 5083-O of 4 mm thick plates.  $Rt/V$ , Welding parameter, which is closely related to welding heat input per unit length of the welded joint affected joint qualities. Peak temperature of FSW joints near stir zone during welding increased with increasing  $Rt/V$ , but lower than solidus temperature for each alloy. As weld defects, lack of bonding and inner defect occurred at low  $Rt/V$  for each alloy, and excess high  $Rt/V$  caused surface tearing as defect both for 2024-T6 and 7075-T6. As to a range of optimum welding condition, 5083-O was wider than those of 2024-T6 and 7075-T6, and optimum  $Rt/V$  range common to three alloys was 3.3 to 5.0. In case of any aluminum alloy, tensile strength of the welded joints increased with increasing  $Rt/V$ , and weld defects caused low tensile strength. The maximum tensile strengths for 2024-T6, 7075-T6 and 5083-O were 373, 444 and 296 MPa in as-welded condition, which were almost 76, 83 and 100 % to base metal strength. Post-weld artificial aging increased the tensile strength of 7075-T6 joint to 512 MPa, 90 % to base metal strength, but in 2024-T6 decreased it slightly.

KEY WORDS: aluminum alloy; high strength aluminum alloy; friction stir welding; weldability; defect; tensile strength; structure; hardness; post-weld aging

## 1. Introduction

Friction Stir Welding (FSW) is a newly developed solid phase welding process.<sup>1)</sup> This process has the advantage of elimination of hot cracking and blowhole, which often occurred by fusion welding such as GTAW or GMAW, and less deformation and shrinkage, no requirement of filler metals and shielding gas, lower peak temperature at the joint during welding due to solid state process.<sup>2, 3)</sup> Therefore it has a potential to join high strength aluminum alloys of 2000 and 7000 series, which are difficult to be fusion welded due to hot cracking. Research works of friction stir welding of these high strength aluminum alloys have been done to evaluate microstructural, mechanical and chemical properties of welded joint for A2024<sup>4, 5)</sup>, A2195<sup>6, 7)</sup> and A7075.<sup>8-10)</sup> However, these works were based on a typical welded joint obtained at a limited condition and no research has been focused on the effect of process parameters on the feature of the welded joint.

The purpose of this study is, including of macro-and microstructural aspects and mechanical properties of FSW joints, to evaluate the effect of welding parameter on weld joint formation by friction stir welding of high strength aluminum alloys of 2024-T6 and 7075-T6 in comparison with 5083-O.

## 2. Experimental procedures

### 2.1 Materials used

Aluminum alloy plates with 100 mm in width, 200 mm in length and 4 mm in thickness were used. Table 1 shows

chemical compositions of aluminum alloys used. A2024 and A7075 are heat treatable alloys and heat treated at T6 conditions. A5083 is the strongest alloy in non-heat treatable alloy and used at annealed condition (O).

Table 1. Chemical compositions of materials used. /mass%

Alloy	Chemical compositions								
	Si	Fe	Cu	Mn	Mg	Cr	Zn	Ti	Al
2024-T6	0.10	0.11	3.92	0.57	1.19	0.01	0.15	0.03	Bal.
5083-O	0.08	0.26	0.02	0.62	4.63	0.08	0.01	0.02	Bal.
7075-T6	0.07	0.17	1.29	0.03	2.11	0.21	5.41	0.02	Bal.

### 2.2 Friction Stir Welding

The process example is schematically shown in Fig.1 and detail procedures were shown in literatures.<sup>2, 3)</sup> A rotating cylindrical tool with a pin on the end, which was set to a spindle of a conventional milling machine, was plunged into aluminum alloy plate just at a weld joint line until a shoulder of the tool touched to the plate surface. Heat generated mainly by friction between the shoulder and plate surface raises the temperature of the joint as high as plastic metal flow can occur around the pin plunged into the plate. Two plates to be welded were fixed on the steel backing plate and were traveled at a preset travel speed to make a continuous butt welded joint. Square-butt joint was made and groove surface was milled. A plate top surface and groove surface were degreased with acetone just prior to welding. As welding parameter, tool rotation speed,  $Rt$  and plate travel speed,  $V$  were changed at 500 to 2500 rpm

and 100 to 1300 mm/min, respectively.

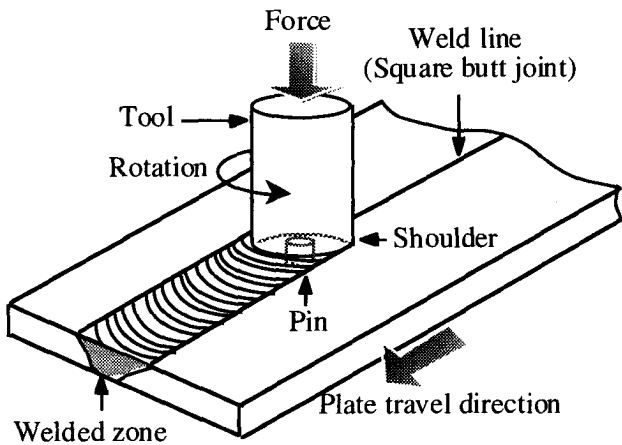


Fig. 1. Schematic illustration of friction stir welding

Peak temperature of the welded joint during welding was measured by a sheathed CA thermocouple in diameter of 0.23 mm, which was inserted into a plate at 2 mm below surface through a small hole at 4 mm from joint center near a rotating pin.

**2.3 Inspection of weld defect**

Visual and X-ray radiography inspections of welded joint were performed to reveal weld defect at the surface and inner zone in the welded joint. Metallurgical inspection was also done on a cross-section of weld joint, which was polished with 0.3 mm in diameter alumina and electrolytically etched with 3 % HBF4 water solution for optical microscopic observations by polarized light.

**2.4 Mechanical property measurement**

Tensile strength of FSW joints were measured using a specimen of as-welded joint surface condition as shown in Fig.2.

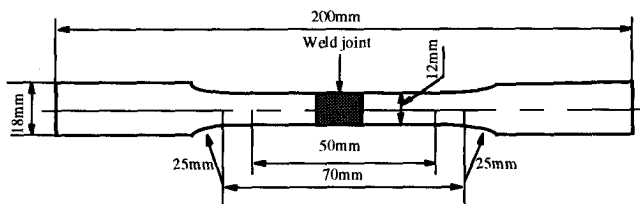


Fig. 2. Tensile test specimen geometry (JIS13B)

Hardness traverse on cross-section of welded joint was measured using a micro-hardness tester at 1.96 N load to A2024 and A7075, 0.98 N load to A5083. Tensile strength and hardness measurements were done at as-welded condition (naturally aged for 30 days) and at post-weld artificially aged condition with 463K, 10 hours for 2024-T6 and 398k, 24 hours for 7075-T6, which are recommended condition by JIS as an aging condition of T6 treatment for base plate.

**3. Results and Discussion**

**3.1 Peak temperature during FSW**

Heat generated during friction stir welding process is by

the frictional interaction of the tool (shoulder and pin surfaces) and by the shear of hot plasticized material in the welded joint.<sup>11)</sup> Tool shoulder heat generation was estimated to be dominant.<sup>12)</sup>

Heat generation by the friction between a cylindrical tool and plate surface is simply explained by equation 1<sup>13)</sup>:

$$Q = \left(\frac{4}{3}\right)\pi^2\mu PR_t D^3 \dots\dots\dots(1)$$

Where Q is the heat generated (W),  $\mu$  is the friction coefficient, P is the pressure (Pa),  $R_t$  is the rotational speed of tool (rotations/s) and D is the surface radius of tool (mm).

According to (1), the heat generated Q is proportional to the tool rotational speed,  $R_t$ . Welding parameter,  $R_t/V$  selected in this study is, therefore, closely related to welding heat input per unit length of the welded joint.

Figure 3 shows the relation between welding parameter  $R_t/V$  and peak temperature of welded joint near the pin during friction stir welding. The peak temperature increased with increasing  $R_t/V$  in each alloy is as expected in the above discussion, and not exceeded solidus temperature for each alloy. This means friction stir welding is solid state welding process. In addition, the difference observed in each alloy suggested the effect of the heat generation by the shear of hot plasticized material during welding, though it was rather small. According to the data from extrusion process<sup>14)</sup>, flow stress of 5083 at elevated temperature and at high strain rate is much higher than those of the others due to higher magnesium content as alloying element, and this may cause more heat generation by the shear.

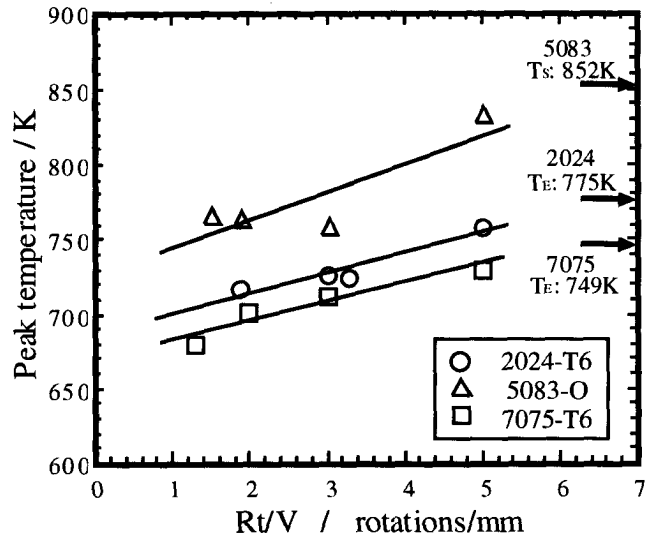


Fig. 3. Relation between welding parameter,  $R_t/V$  and peak temperature of welded joint during FSW

**3.2 Weld formation**

Quality of FSW joints grouped into five typical types by visual appearance and X-ray radiography inspection. Figure 4 shows the relation between welding parameter and joint quality on each alloy. In any case, weld defects were dominantly observed at lower  $R_t/V$ . In excess high value of welding parameter, surface tearing and inner defect were again observed on 2024-T6 and 7075-T6 alloy, respectively.

This may be caused by grain boundary liquation due to comparatively low eutectic temperature,  $T_E$  of these alloys as shown in Fig.4. Therefore, optimum Rt/V value range showing good FSW joints was 3.3 to 5.0 in an intermediate condition. Also, 5083-O alloy indicated the range of optimum welding condition was wider than those of 2024-T6 or 7075-T6.

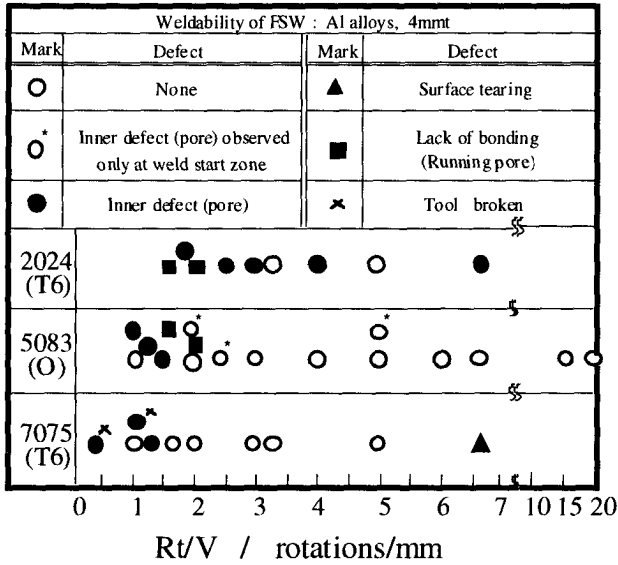


Fig. 4. Relation between welding parameter and joint quality

Typical appearance of weld surface, X-ray radiography and microscopic structure on cross-section of FSW joint with and without weld defects are shown in Fig.5 in top, middle and bottom columns, respectively.

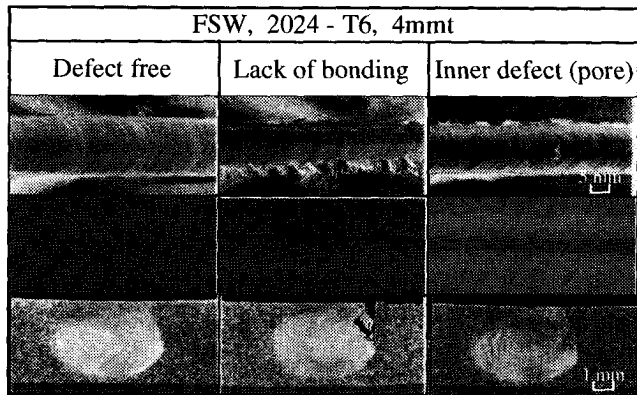


Fig. 5. Appearance and X-ray radiography of FSW joint

Defect free joints were made at the adequate conditions. As a weld defect, three types of defect were observed. The most severe one is a lack of bonding, which is a groove-like or a running pore defect, made along the boundary between a stir zone and HAZ at advancing side, and appeared on the top surface. Another is an inner defect, which is invisible, but can be detected by X-ray radiography, and was consisted of many small voids, and formed in stir zone near surface at advancing side. The formation mechanism of these two types of defect is not clear yet. The shear motion due to the opposite direction for each other between metal

flow around a rotating pin and a traveling base plate at the advancing side caused these defects, when temperature rise was not high enough to make a good metal bonding. The other is kissing bond, which had less than 50 to 100  $\mu\text{m}$  in size, was occasionally formed in the root site at low Rt/V due to an inadequate plunge depth of the pin. However, the great effect of kissing bond upon the joint strength would be disregarded.

### 3.3 Hardness traverse measurement

The hardness traverse of FSW joints measured at as-welded and post-weld artificial aging condition are presented in Fig.6 collectively for each alloy, and it has been correlated spatially with different weld regions.

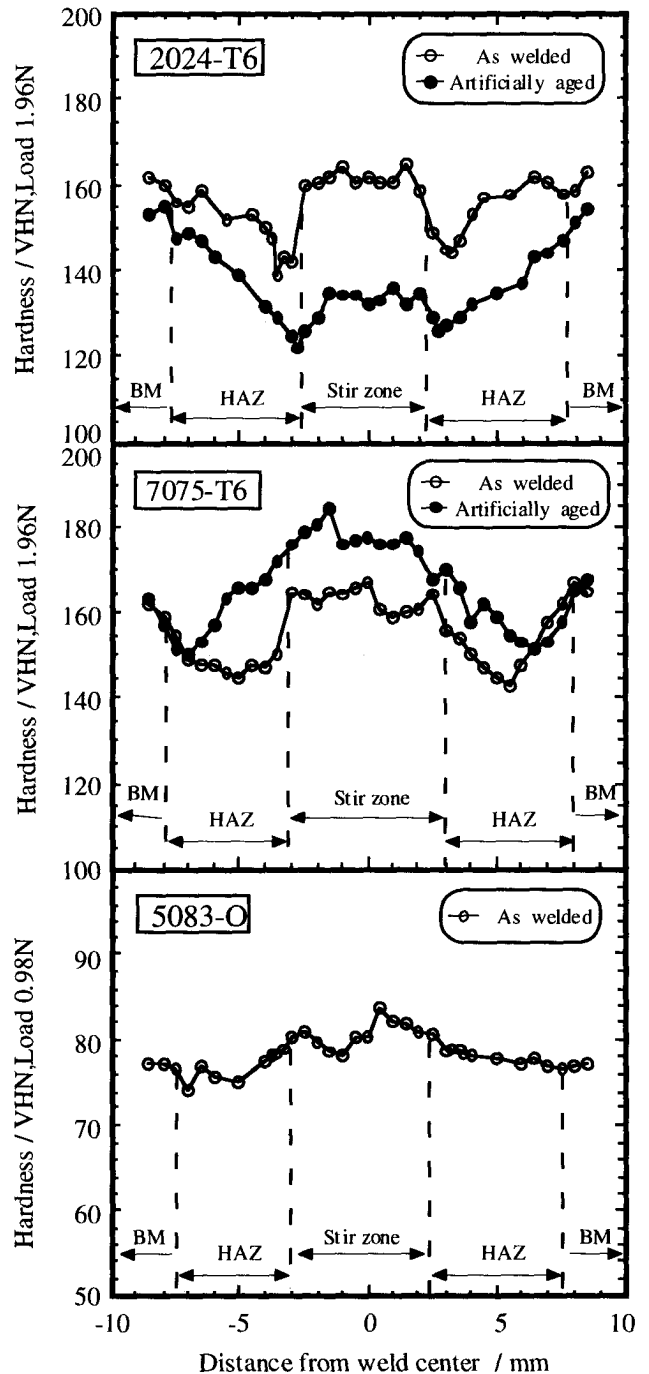


Fig. 6. Microhardness traverse on FSW joints

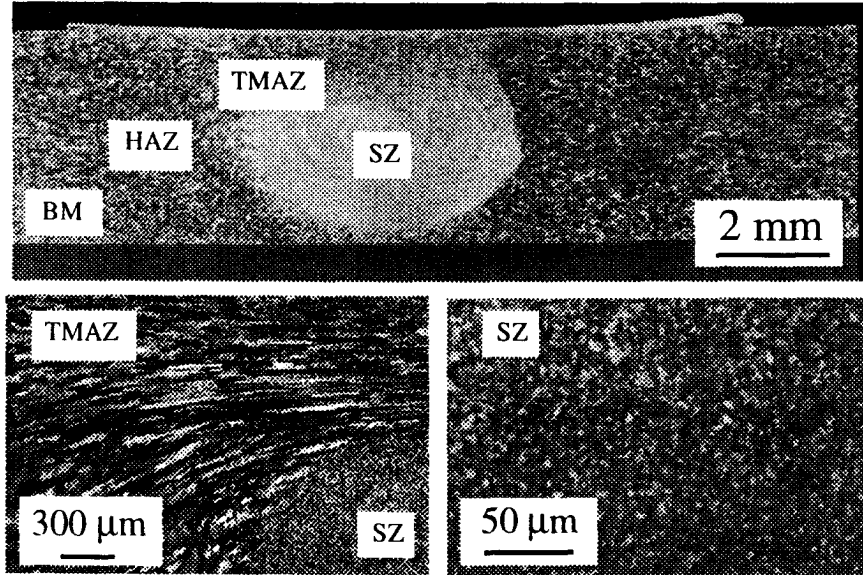


Fig. 7. Typical macro- and microstructure on cross-section of FSW joint, 2024-T6

Figure 7 shows the macro- and microstructures of a transverse cross-section taken through a weld made in alloy 2024-T6. Several microstructurally distinct regions include the base metal as well as the stir zone, the heat affected zone (HAZ) and the thermo-mechanically affected zone (TMAZ). The stir zone is fully recrystallized and very fine equiaxed grains with several  $\mu\text{m}$  in diameter is produced by dynamic recrystallization.<sup>8)</sup>

Quite similar structures were observed in the other alloys. Based on the hardness traverse measurement, base metal and stir zone were almost same values 155 to 160 VHN, but in the regions of the HAZ the large drop was seen in hardness to 140 VHN for 2024-T6 or 7075-T6 alloy. 7075-T6 was increased by post-weld aging treatment, in contrast, it caused decreasing hardness traverse of 2024-T6 due to over-aging. 5083-O had 75 to 80 VHN for whole hardness traverse. No large drop in the regions of HAZ was observed in comparison with 2024-T6 or 7075-T6 due to non-heat treatable and annealed condition of the base plate.

### 3.4 Tensile strength test

Figures 8, 9 and 10 show relation between welding parameter and tensile strength of FSW joints in relation to joint efficiency for each alloy. In case of any aluminum alloy, tensile strength of joints increased with increasing welding parameter, and weld defects caused apparently low tensile strength. All good joints had high strength, almost 100 % for 5083-O, about 80 % for 2024-T6 and 7075-T6 in joint efficiency to base metal strength even as-welded condition. Kissing bond, occasionally observed at low Rt/V caused the slight decrease in tensile strength typically in 5083-O and 7075-T6. Post-weld artificially aged 7075-T6 alloy showed higher strength than that of as-welded condition and high joint efficiency of 90%, but 2024-T6 showed slight decrease due to over-aging. Certainly, the tensile test results of 2024-T6 and 7075-T6 on post-weld aged condition correlated to hardness traverse in the same pattern.

Fracture position in welded joints with defect free condition was in HAZ in each alloy.

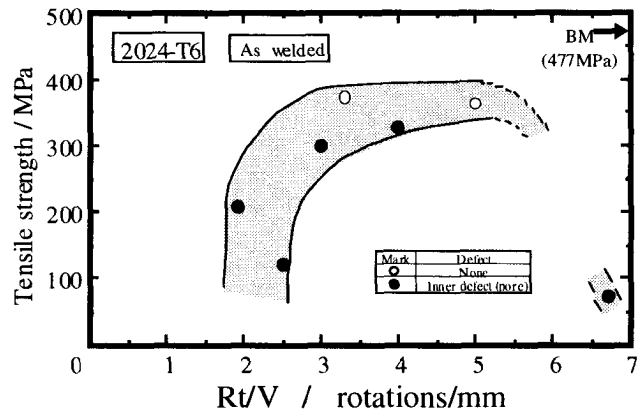


Fig. 8. Effect of welding parameter on tensile strength of FSW joint, 2024-T6

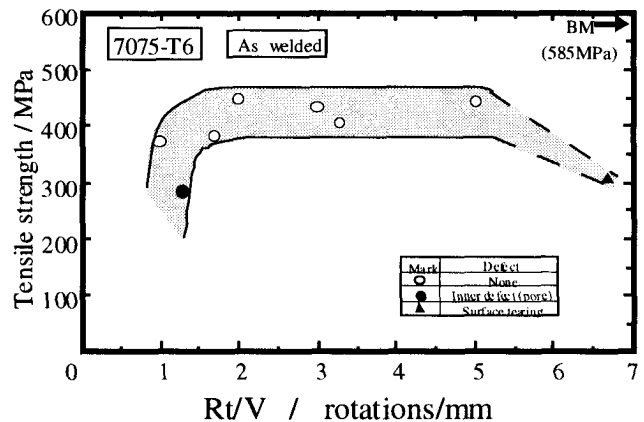


Fig. 9. Effect of welding parameter on tensile strength of FSW joint, 7075-T6

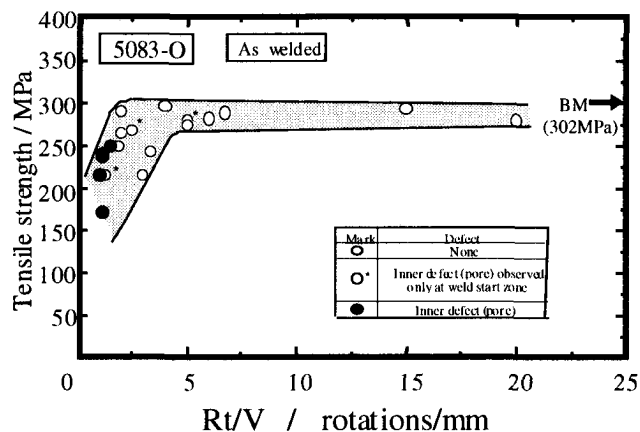


Fig. 10. Effect of welding parameter on tensile strength of FSW joint, 5083-O

#### 4. Conclusion

In this study, the effects of welding parameter on weld formation and the mechanical properties correlated microstructural aspects of FSW joints have been evaluated for high strength aluminum alloys of 2024-T6 and 7075-T6 in comparison with 5083-O of 4 mm thick plates. Based on our analysis, we can summarize the following conclusions.

- (1) Rt/V, the Welding parameter, which is closely related to welding heat input per unit length of the welded joint affected joint qualities. Peak temperature of FSW joints near stir zone during welding increased with increasing Rt/V, but lower than solidus temperature for each alloy.
- (2) As weld defects, lack of bonding and inner defect occurred at low Rt/V caused surface tearing as defect also for 2024-T6 and 7075-T6.
- (3) As to a range of optimum welding condition, 5083-O was wider than those of 2024-T6 and 7075-T6, and optimum Rt/V range common to three alloys was 3.3 to 5.0.
- (4) Tensile strength of the welded joints increased with increasing Rt/V, and weld defects caused low tensile strength. The maximum tensile strengths for 2024-T6, 7075-T6 and 5083-O were 373, 444 and 296 MPa in as-welded condition, which were almost 76, 83 and 100 % to base metal strength. Post-weld artificial aging increased the tensile strength of 7075-T6 joint to 512 MPa, 90 % to base metal strength, but decreased that of 2024-T6 slightly.

#### REFERENCES

- 1) W.M.Thomas et al: International Patent Application No. PCT/GB92/02203 and GB Patent Application No. 9125978.8, 6 Dec.1991, U.S. Patent No.5,460,317.
- 2) C.J.Dawes: Proc.of the 6<sup>th</sup> Int. Symp.JWS, (1996), 711.
- 3) C.J.Dawes and W.M.Thomas: Weld. J., 75 (1996), 41.
- 4) G.Bussu and P.E.Irving: 1<sup>st</sup> Int. Symp. On Friction Stir Welding, TWI, (1999), (CD-ROM).
- 5) G.Biallas, R.Braun, C.D.Donne, G.Staniek and W.A. Kaysser: 1<sup>st</sup> Int. Symp. On Friction Stir Welding, TWI, (1999), (CD-ROM).

- 6) R.J.Ding and P.A.Oelgoetz: 1<sup>st</sup> Int. Symp. On Friction Stir Welding, TWI, (1999), (CD-ROM).
- 7) D.Kinchen, Z.Li and G.Adams: 1<sup>st</sup> Int. Symp. On Friction Stir Welding, TWI, (1999), (CD-ROM).
- 8) C.G.Rhodes, M.W.Mahoney, W.H.Bingel, R.A.Spurling and C.C.Bampton: Script. Met., 36 (1997), 69.
- 9) M.W.Mahoney, C.G.Rhodes, J.G.Flintoff, R.A.Spurling and W.H. Bingel: Metall. And Mate. Trans. A, 29A (1998), 1955.
- 10) J.Lumsden III, M.Mahoney, G.Pollock, D.Waldron and A. Guinasso: 1<sup>st</sup> Int. Symp. On Friction Stir Welding, TWI, (1999), (CD-ROM).
- 11) M.J.Russel, H.R.Shercliff: Proc.of INALCO`98, (1998), 185.
- 12) M.J.Russell, H.R.Shercliff: 1<sup>st</sup> Int. Symp. On Friction Stir Welding, TWI, (1999), (CD-ROM).
- 13) O.Frigaard, O.Grong and O.T.Midling: Proc.of INALCO`98, (1998), 197.
- 14) K.Laue and H.Stenger: Extrusion, AMS, (1981), 45.